PTEP

Prog. Theor. Exp. Phys. **2021**, 093B05 (14 pages)
DOI: 10.1093/ptep/ptab106

One-loop W boson contributions to the decay $H \to Z\gamma$ in the general R_ξ gauge

Khiem Hong Phan[1,2,*], Le Tho Hue[3], and Dzung Tri Tran[4]

[1]*Institute of Fundamental and Applied Sciences, Duy Tan University, Ho Chi Minh City 700000, Vietnam*
[2]*Faculty of Natural Sciences, Duy Tan University, Da Nang City 550000, Vietnam*
[3]*Institute of Physics, Vietnam Academy of Science and Technology, 10 Dao Tan, Ba Dinh, Hanoi, Vietnam*
[4]*University of Science Ho Chi Minh City, 227 Nguyen Van Cu, District 5, Ho Chi Minh City, Vietnam*
*E-mail: phanhongkhiem@duytan.edu.vn

Received July 1, 2021; Accepted August 4, 2021; Published August 11, 2021

One-loop W boson contributions to the decay $H \to Z\gamma$ in the general R_ξ gauge are presented. The analytical results are expressed in terms of well-known Passarino–Veltman functions such that their numerical evaluations can be generated using `LoopTools`. In the limit $d \to 4$, we have shown that these analytical results are independent of the unphysical parameter ξ and consistent with previous results. The gauge parameter independence is also checked numerically for consistence. Our results are also well stable with different values of $\xi = 0,\ 1,\ 100$ and $\xi \to \infty$.

Subject Index B53, B59

1. Introduction

The decay process of the standard model-like (SM-like) Higgs boson $H \to Z\gamma$ is of great interest at the Large Hadron Collider (LHC) as well as future colliders [1–4]. Similar to the important loop-induced decay $H \to \gamma\gamma$, which is one of the key channels for finding the SM-like Higgs boson at the LHC, the partial decay width of the decay $H \to Z\gamma$ will provide important information on the nature of the Higgs sector. Since the leading contributions to this decay amplitude are from one-loop Feynman diagrams, it is sensitive to new physics predicted by many beyond the standard models (BSM), i.e., new contributions of many new heavy charged particles that exchange in the loop diagrams. Therefore, detailed calculations for one-loop and higher-loop contributions to the decay channel $H \to Z\gamma$ are necessary.

There have been many computations for one-loop contributions to the decay channel $H \to Z\gamma$ within SM and its extensions in Ref. [5–24], also in the references therein. In Ref. [25], the authors proposed the dispersion theoretic evaluations for $H \to Z\gamma$. In addition, hypergeometric presentation for one-loop contribution to the amplitude of the decay $H \to Z\gamma$ has been presented in Ref. [26]. Most of the calculations were carried out in the unitary gauge because of the lesser number of the Feynman diagrams in this gauge than in the other ones. However, the results may experience problems relating to the large numerical cancellations, especially the higher-rank tensor one-loop integrals that occur in the diagrams due to the W boson exchange. In our opinion, the derivation the one-loop W boson contributions to the decay amplitude $H \to Z\gamma$ in the general R_ξ gauge is mandatory, even in the SM framework. This helps to verify the correctness of the final results supposed to be independent of the unphysical parameter ξ. Furthermore, one can obtain a good stability of the results by fixing suitable values of ξ.

Funded by SCOAP[3]

Many recent BSMs are electroweak gauge extensions, such as the left–right models (LR) constructed from the $SU(2)_L \times SU(2)_R \times U(1)_Y$ [27–29], the 3-3-1 models $(SU(3)_L \times U(1)_X)$ [30–36], the 3-4-1 models $(SU(4)_L \times U(1)_X)$ [35], etc. They all predict new charged gauge bosons which may give considerable one-loop contributions to the decay amplitude $H \to Z\gamma$. Once their couplings and the respective Goldstone bosons and ghosts particles are determined, their contributions to the decay amplitude $H \to Z\gamma$ can be presented analytically using the results given in this paper, although it is limited in the standard model framework. They can be used to cross-check with other results calculated in the unitary gauge [20]. This is another way to confirm the complicated properties of the couplings related with new Goldstone bosons appearing in the BSM.

For the above reasons, detailed calculations for one-loop W boson contributions to $H \to Z\gamma$ in the R_ξ gauge will be presented in this paper. The analytical results will be grouped in form factors that are written in terms of the Passarino–Veltman functions so that their numerical evaluations can be generated by `LoopTools` [37]. In the limit $d \to 4$, the analytic results will be used to check for the ξ-independence and confirm previous results. Numerical checks for the ξ-independence of the form factors will be also discussed. The stability of results will be tested by varying $\xi = 0,\ 1,\ 100$ and $\xi \to \infty$.

The layout of the paper is as follows: In Sect. 2, we briefly present the one-loop tensor reduction method. Notations for one-loop form factors contributing to the amplitude of the SM-like Higgs decay into a Z boson and a photon will be defined before listing all analytical results in that section. Conclusions and outlook are given in Sect. 3. In the appendix, Feynman rules for the decay channel are discussed.

2. Calculations

In general, one-loop decay amplitude is decomposed into one-loop tensor integrals which can be reduced frequently to the final forms, which are sums of only scalar functions. Our calculation will follow the tensor reduction method for one-loop integrals developed in Ref. [38]. This technique is described briefly in the following.

The notations of one-loop one-, two- and three-point tensor integrals with rank P are given by

$$\{A; B; C\}^{\mu_1\mu_2\cdots\mu_P} = \int \frac{d^d k}{(2\pi)^d} \frac{k^{\mu_1} k^{\mu_2} \ldots k^{\mu_P}}{\{D_1; D_1D_2; D_1D_2D_3\}}. \tag{1}$$

In this formula, D_j $(j = 1, 2, 3)$ are the inverse Feynman propagators

$$D_j = (k + q_j)^2 - m_j^2 + i\rho, \tag{2}$$

$q_j = \sum_{i=1}^{j} p_i$, p_i are the external momenta, and m_j are internal masses in the loops.

The explicit reduction formulas for one-loop one-, two- and three-points tensor integrals up to rank $P = 3$ are written as follows [38]:

$$A^\mu = 0, \tag{3}$$

$$A^{\mu\nu} = g^{\mu\nu} A_{00}, \tag{4}$$

$$A^{\mu\nu\rho} = 0, \tag{5}$$

$$B^\mu = q^\mu B_1, \tag{6}$$

$$B^{\mu\nu} = g^{\mu\nu} B_{00} + q^\mu q^\nu B_{11}, \tag{7}$$

$$B^{\mu\nu\rho} = \{g,q\}^{\mu\nu\rho} B_{001} + q^\mu q^\nu q^\rho B_{111}, \tag{8}$$

$$C^\mu = q_1^\mu C_1 + q_2^\mu C_2 = \sum_{i=1,2} q_i^\mu C_i, \tag{9}$$

$$C^{\mu\nu} = g^{\mu\nu} C_{00} + \sum_{i,j=1,2} q_i^\mu q_j^\nu C_{ij}, \tag{10}$$

$$C^{\mu\nu\rho} = \sum_{i=1}^{2} \{g,q_i\}^{\mu\nu\rho} C_{00i} + \sum_{i,j,k=1}^{2} q_i^\mu q_j^\nu q_k^\rho C_{ijk}. \tag{11}$$

For convenience, the short notation [38] $\{g,q_i\}^{\mu\nu\rho}$ will be used as follows: $\{g,q_i\}^{\mu\nu\rho} = g^{\mu\nu} q_i^\rho + g^{\nu\rho} q_i^\mu + g^{\mu\rho} q_i^\nu$. Following this approach, the scalar coefficients $A_{00}, B_1, \cdots, C_{222}$ in the right-hand sides of the above equations are so-called Passarino–Veltman functions [38]. Their analytic formulas for numerical calculations are well-known. More conveniently, these functions can be calculated numerically using the available package `LoopTools` [37].

The above notations will be used to evaluate the one-loop W contributions to the decay amplitude $H \to Z(p_1)\gamma(p_2)$. In the SM framework, these contributions come from the Feynman diagrams given in Fig. A.1, where all W boson, Goldstone boson and ghost particles exchanging in the loop must be considered in the general R_ξ gauge.

The total amplitude of the decay channel is then expressed in terms of the Lorentz invariant structure as follows:

$$\mathcal{A}_{H\to Z\gamma} = \mathcal{A}_{\mu\nu} \epsilon_\mu^*(p_1) \epsilon_\nu^*(p_2) = \left\{ \mathcal{A}_{00} g^{\mu\nu} + \sum_{i,j=1}^{2} \mathcal{A}_{ij} p_i^\mu p_j^\nu \right\} \epsilon_\mu^*(p_1) \epsilon_\nu^*(p_2). \tag{12}$$

All kinematic invariant variables are relevant in this process:

$$p_1^2 = M_Z^2, \tag{13}$$

$$p_2^2 = 0, \tag{14}$$

$$p^2 = (p_1 + p_2)^2 = M_H^2, \tag{15}$$

which results in a consequence that

$$p_1 p_2 = \frac{M_H^2 - M_Z^2}{2}. \tag{16}$$

The Ward identity $p_2^\nu \epsilon_\nu^*(p_2) = 0$ implies that the two form factors $\mathcal{A}_{22}$ and $\mathcal{A}_{12}$ do not contribute to the amplitude given in Eq. (12). In addition, we have $p_2^\nu \mathcal{A}_{\mu\nu} = 0$, leading to another zero form factor, namely $\mathcal{A}_{11} = 0$. Now, the amplitude has a very simple form:

$$\mathcal{A}_{H\to Z\gamma} = \left\{ \mathcal{A}_{00} g^{\mu\nu} + \mathcal{A}_{21} p_1^\nu p_2^\mu \right\} \epsilon_\mu^*(p_1) \epsilon_\nu^*(p_2). \tag{17}$$

The form factors $\mathcal{A}_{00}, \mathcal{A}_{21}$ will be expressed in terms of the Passarino–Veltman functions mentioned in the beginning of this section. The derivations are performed with the help of `Package-X` [39] for handling all Dirac traces in d dimensions. One-loop form factors are presented in the standard notation defined in `LoopTools` [37] on a diagram-by-diagram basis.

2.1. *In the general R_ξ gauge*

We first carry out the calculations in the general R_ξ gauge. To simplify the computations, the W boson propagator is decomposed into the following form:

$$\frac{-i}{k^2-M_W^2}\left[g^{\mu\nu}-(1-\xi)\frac{k^\mu k^\nu}{k^2-M_\xi^2}\right]=\frac{-i}{k^2-M_W^2}\left(g^{\mu\nu}-\frac{k^\mu k^\nu}{M_W^2}\right)+\frac{-i}{k^2-M_\xi^2}\frac{k^\mu k^\nu}{M_W^2}, \quad (18)$$

with $M_\xi^2 = \xi M_W^2$. The first term in the right-hand side of Eq. (18) is nothing but the W boson propagator in the unitary gauge, while the second term relates to the propagators of Goldstone bosons and ghost particles. In the convention of Eq. (18), each diagram with a W boson exchanging in the loop will be separated into several parts. For example, the Feynman amplitude for diagram (a) in Fig. A.1 is divided into 8 terms as follows:

$$\mathcal{A}^{(a)} = \sum_{i,j,k=1}^{2} \mathcal{A}_{ijk}^{(a)}. \quad (19)$$

The notation $\mathcal{A}_{ijk}^{(a)}$ corresponds to which term on the right-hand side of Eq. (18) is taken. In this scheme, the amplitude in Eq. (17) is presented by means of

$$\mathcal{A}_{H\to Z\gamma} = \left\{\left[\sum_{\text{diag}\equiv\{a,\cdots,j\}} \mathcal{A}_L^{(\text{diag})}(\xi)\right] g^{\mu\nu} + \left[\sum_{\text{diag}\equiv\{a,\cdots,j\}} \mathcal{A}_T^{(\text{diag})}(\xi)\right] p_2^\mu p_1^\nu\right\} \epsilon_\mu^*(p_1)\epsilon_\nu^*(p_2) \quad (20)$$

The terms $\mathcal{A}_L^{(\text{diag})}(\xi)$ and $\mathcal{A}_T^{(\text{diag})}(\xi)$ will be collected on a diagram-by-diagram basis in the following subsections. In this article, we show analytic results for $\mathcal{A}_T^{(\text{diag})}(\xi)$ as examples.

2.1.1. *Diagrams a and a′*

We first calculate the topologies $(a + a')$ having only W boson in the loop diagrams (see the two diagrams a and a' in Fig. A.1). The respective form factors denoted in Eq. (20) are split into 8 pieces, namely

$$\mathcal{A}_T^{(a+a')}(\xi) = \frac{g_{HWW}g_{ZWW}g_{AWW}}{32\pi^2 M_W^4}\Big\{\mathcal{A}_{111}^T(\xi)+\mathcal{A}_{112}^T(\xi)+\mathcal{A}_{121}^T(\xi)+\mathcal{A}_{211}^T(\xi)+\mathcal{A}_{122}^T(\xi) + \mathcal{A}_{212}^T(\xi)+\mathcal{A}_{221}^T(\xi)+\mathcal{A}_{222}^T(\xi)\Big\}. \quad (21)$$

All terms in the above equation are presented in terms of the Passarino–Veltman functions as follows:

$$\begin{aligned}\mathcal{A}_{111}^T(\xi) = {} & (2M_H^2+4M_W^2)\Big[B_{11}+B_1\Big](M_H^2,M_W^2,M_W^2) + 4M_W^2 B_0(M_H^2,M_W^2,M_W^2)\\ & + 8M_W^2(4M_W^2-M_Z^2)C_0(M_H^2,M_Z^2,0,M_W^2,M_W^2,M_W^2)\\ & + 2\Big[2M_H^2(2M_W^2-M_Z^2)+8(d-1)M_W^4-4M_W^2M_Z^2\Big]\\ & \times[C_{22}+C_{12}+C_2](M_Z^2,0,M_H^2,M_W^2,M_W^2,M_W^2), \end{aligned} \quad (22)$$

$$\begin{aligned}\mathcal{A}_{112}^T(\xi) = {} & -4M_W^2B_0(M_H^2,M_W^2,M_\xi^2)+(6M_W^2M_Z^2-8M_W^4)C_0(M_Z^2,0,M_H^2,M_W^2,M_W^2,M_\xi^2)\\ & + 2M_W^2M_Z^2C_1(M_Z^2,0,M_H^2,M_W^2,M_W^2,M_\xi^2)+[M_H^2-M_W^2(\xi-1)]\end{aligned}$$

$$\times \Big\{(3M_Z^2 - 4M_W^2)\Big[C_{22} + C_{12}\Big](M_Z^2, 0, M_H^2, M_W^2, M_W^2, M_\xi^2) - 2B_{11}(M_H^2, M_W^2, M_\xi^2)\Big\} + [M_H^2 - M_W^2(\xi - 3)] \times \Big[- 2B_1(M_H^2, M_W^2, M_\xi^2) - (4M_W^2 - 3M_Z^2)C_2(M_Z^2, 0, M_H^2, M_W^2, M_W^2, M_\xi^2)\Big], \quad (23)$$

$$\mathcal{A}_{121}^T(\xi) = 2M_H^2(M_Z^2 - M_W^2)\Big[C_{22} + C_{12} + C_2\Big](M_Z^2, 0, M_H^2, M_W^2, M_\xi^2, M_W^2) + 4M_W^2(M_Z^2 - M_W^2)\Big[C_{22} + C_{12} + C_2 + C_1 + C_0\Big](M_Z^2, 0, M_H^2, M_W^2, M_\xi^2, M_W^2), \quad (24)$$

$$\mathcal{A}_{211}^T(\xi) = [M_W^2(\xi + 1) - M_H^2] \times \Big\{2B_1(M_H^2, M_\xi^2, M_W^2) + (4M_W^2 - 3M_Z^2)C_1(M_H^2, M_Z^2, 0, M_\xi^2, M_W^2, M_W^2)\Big\} + 4M_W^2(2M_W^2 - M_Z^2)C_1(M_Z^2, 0, M_H^2, M_\xi^2, M_W^2, M_W^2) + [M_H^2 - M_W^2(\xi - 1)] \times \Big\{(3M_Z^2 - 4M_W^2)\Big[C_{22} + C_{12}\Big](M_Z^2, 0, M_H^2, M_\xi^2, M_W^2, M_W^2) - 2B_{11}(M_H^2, M_\xi^2, M_W^2)\Big\}, \quad (25)$$

$$\mathcal{A}_{122}^T(\xi) = M_Z^2[M_W^2(\xi - 1) - M_H^2]\Big[C_{12} + C_{11}\Big](M_H^2, M_Z^2, 0, M_W^2, M_\xi^2, M_\xi^2) - 2M_Z^2M_W^2\Big[C_2 + C_0\Big](M_H^2, M_Z^2, 0, M_W^2, M_\xi^2, M_\xi^2) - M_Z^2[M_H^2 - M_W^2(\xi - 3)]C_1(M_H^2, M_Z^2, 0, M_W^2, M_\xi^2, M_\xi^2), \quad (26)$$

$$\mathcal{A}_{212}^T(\xi) = 2(M_H^2 - 2M_\xi^2)\Big[B_{11} + B_1\Big](M_H^2, M_\xi^2, M_\xi^2) + 2(M_W^2 - M_Z^2)(M_H^2 - 2M_\xi^2)\Big[C_{22} + C_{12} + C_2\Big](M_Z^2, 0, M_H^2, M_\xi^2, M_W^2, M_\xi^2), \quad (27)$$

$$\mathcal{A}_{221}^T(\xi) = M_Z^2[M_W^2(\xi + 1) - M_H^2]C_2(M_Z^2, 0, M_H^2, M_\xi^2, M_\xi^2, M_W^2) + M_Z^2[M_W^2(\xi - 1) - M_H^2]\Big[C_{22} + C_{12}\Big](M_Z^2, 0, M_H^2, M_\xi^2, M_\xi^2, M_W^2), \quad (28)$$

$$\mathcal{A}_{222}^T(\xi) = 0. \quad (29)$$

2.1.2. Diagram b

We next consider the topology *b* which has two W boson internal lines. The one-loop form factors read as

$$\mathcal{A}_{11}^T(\xi) = \Big[M_H^2B_{111} + 2B_{001} + (M_H^2 - M_W^2)B_{11} + B_{00} - M_W^2(B_1 + B_0)\Big](M_H^2, M_W^2, M_W^2), \quad (30)$$

$$\mathcal{A}_{12}^T(\xi) = \Big[M_W^2(B_0 + B_1) - B_{00} - M_H^2(B_{11} + B_{111}) - 2B_{001}\Big](M_H^2, M_W^2, M_\xi^2), \quad (31)$$

$$\mathcal{A}_{21}^{T}(\xi) = \Big[[M_W^2(1-\xi) - M_H^2]B_{11} - M_\xi^2 B_1 - M_H^2 B_{111} - B_{00} - 2B_{001}\Big](M_H^2, M_\xi^2, M_W^2), \quad (32)$$

$$\mathcal{A}_{22}^{T}(\xi) = \Big[(M_H^2 + M_\xi^2)B_{11} + M_\xi^2 B_1 + M_H^2 B_{111} + B_{00} + 2B_{001}\Big](M_H^2, M_\xi^2, M_\xi^2). \quad (33)$$

2.1.3. Diagrams c and c′

The form factors due to the triangle diagrams that have two W bosons and a Goldstone boson in the loop are considered next. They are expressed in the same scheme:

$$\mathcal{A}_{T}^{(c+c')}(\xi) = \mathcal{A}_{110}^{T}(\xi) + \mathcal{A}_{120}^{T}(\xi) + \mathcal{A}_{210}^{T}(\xi) + \mathcal{A}_{220}^{T}(\xi). \quad (34)$$

The related terms in the above equation are shown:

$$\begin{aligned}
\mathcal{A}_{110}^{T}(\xi) = {} & \frac{g_{HWX}g_{ZWW}g_{AWX}}{8\pi^2 M_W^4}\Big\{2M_W^2(2M_W^2 - M_Z^2)C_0(M_Z^2, 0, M_H^2, M_W^2, M_W^2, M_\xi^2) \\
& - 2M_W^2 M_Z^2 C_1(M_Z^2, 0, M_H^2, M_W^2, M_W^2, M_\xi^2) \\
& + (2M_W^2 - M_Z^2)[M_H^2 - M_W^2(\xi-1)]\Big[C_{12} + C_{22}\Big](M_Z^2, 0, M_H^2, M_W^2, M_W^2, M_\xi^2) \\
& + (2M_W^2 - M_Z^2)[M_H^2 - M_W^2(\xi-3)]C_2(M_Z^2, 0, M_H^2, M_W^2, M_W^2, M_\xi^2)\Big\} \\
& + \frac{g_{HWX}g_{AWW}g_{ZWX}}{8\pi^2 M_W^4}\Big\{4M_W^4 C_0(M_H^2, M_Z^2, 0, M_W^2, M_\xi^2, M_W^2) \\
& + 2M_W^2[M_H^2 - M_W^2(\xi-1)]\Big[C_{12} + C_{11}\Big](M_H^2, M_Z^2, 0, M_W^2, M_\xi^2, M_W^2) \\
& + 2M_W^2[M_H^2 - M_W^2(\xi-3)]C_1(M_H^2, M_Z^2, 0, M_W^2, M_\xi^2, M_W^2)\Big\}, \quad (35)
\end{aligned}$$

$$\begin{aligned}
\mathcal{A}_{120}^{T}(\xi) = {} & \frac{g_{HWX}g_{ZWW}g_{AWX}}{8\pi^2 M_W^4}\Big\{(M_W^2 - M_Z^2)[M_W^2(\xi-3) - M_H^2]C_2(M_Z^2, 0, M_H^2, M_W^2, M_\xi^2, M_\xi^2) \\
& + (M_Z^2 - M_W^2)[M_H^2 - M_W^2(\xi-1)]\Big[C_{22} + C_{12}\Big](M_Z^2, 0, M_H^2, M_W^2, M_\xi^2, M_\xi^2) \\
& + 2M_W^2(M_Z^2 - M_W^2)\Big[C_1 + C_0\Big](M_Z^2, 0, M_H^2, M_W^2, M_\xi^2, M_\xi^2)\Big\} \\
& + \frac{g_{HWX}g_{AWW}g_{ZWX}}{8\pi^2 M_W^4}\Big\{M_W^2[M_W^2(\xi-3) - M_H^2]C_1(M_H^2, M_Z^2, 0, M_W^2, M_\xi^2, M_\xi^2) \\
& - M_W^2[M_H^2 - M_W^2(\xi-1)]\Big[C_{12} + C_{11}\Big](M_H^2, M_Z^2, 0, M_W^2, M_\xi^2, M_\xi^2) \\
& - 2M_W^4\Big[C_2 + C_0\Big](M_H^2, M_Z^2, 0, M_W^2, M_\xi^2, M_\xi^2)\Big\}, \quad (36)
\end{aligned}$$

$$\begin{aligned}
\mathcal{A}_{210}^{T}(\xi) = {} & \frac{g_{HWX}g_{ZWW}g_{AWX}}{8\pi^2 M_W^4}\Big\{(M_\xi^2 - M_H^2)(M_W^2 - M_Z^2) \\
& \times \Big[C_{22} + C_{12} + C_2\Big](M_Z^2, 0, M_H^2, M_\xi^2, M_W^2, M_\xi^2)\Big\} \\
& + \frac{g_{HWX}g_{AWW}g_{ZWX}}{8\pi^2 M_W^4}\Big\{(M_\xi^2 - M_H^2)M_W^2 \\
& \times \Big[C_{12} + C_{11} + C_1\Big](M_H^2, M_Z^2, 0, M_\xi^2, M_\xi^2, M_W^2)\Big\}, \quad (37)
\end{aligned}$$

$$\mathcal{A}^T_{220}(\xi) = \frac{g_{HWX}g_{ZWW}g_{AWX}}{8\pi^2 M_W^4}\Big\{M_Z^2(M_\xi^2 - M_H^2)\Big[C_{22} + C_{12} + C_2\Big](M_Z^2, 0, M_H^2, M_\xi^2, M_\xi^2, M_\xi^2)\Big\}. \quad (38)$$

2.1.4. Diagrams d and d′

We are now going to consider one-loop two-point diagrams with exchanging a W boson and a Goldstone boson in the loop (see diagrams d and d' in Fig. A1). The form factors are divided into two parts as follows:

$$\mathcal{A}_T^{(d+d')}(\xi) = \mathcal{A}^T_{10}(\xi) + \mathcal{A}^T_{20}(\xi). \quad (39)$$

All components in the equation are given:

$$\mathcal{A}^T_{10}(\xi) = 0, \quad (40)$$

$$\mathcal{A}^T_{20}(\xi) = \frac{g_{HZWX}g_{AWX}}{8\pi^2 M_W^2}\Big[B_{00} - M_W^2 B_0\Big](0, M_W^2, M_\xi^2) + \frac{g_{HAWX}g_{ZWX}}{8\pi^2 M_W^2}\Big[B_{00} - M_W^2 B_0\Big](M_Z^2, M_\xi^2, M_W^2). \quad (41)$$

2.1.5. Diagrams e and e′

One-loop topologies with two Goldstone bosons and one W boson in internal lines are considered. The form factors are written as

$$\mathcal{A}_T^{(e+e')}(\xi) = \frac{g_{HWX}(g_{ZWX}g_{AXX} + g_{AWX}g_{ZXX})}{4\pi^2 M_W^2}\Big[\mathcal{A}^T_{100}(\xi) + \mathcal{A}^T_{200}(\xi)\Big]. \quad (42)$$

The related terms in the equation are decomposed as

$$\mathcal{A}^T_{100}(\xi) = [M_H^2 + M_W^2(3-\xi)]C_2(M_Z^2, 0, M_H^2, M_W^2, M_\xi^2, M_\xi^2) + 2M_W^2\Big[C_0 + C_1\Big](M_Z^2, 0, M_H^2, M_W^2, M_\xi^2, M_\xi^2) + [M_H^2 + M_W^2(1-\xi)]\Big[C_{22} + C_{12}\Big](M_Z^2, 0, M_H^2, M_W^2, M_\xi^2, M_\xi^2), \quad (43)$$

$$\mathcal{A}^T_{200}(\xi) = (M_\xi^2 - M_H^2)\Big[C_{22} + C_{12} + C_2\Big](M_Z^2, 0, M_H^2, M_\xi^2, M_\xi^2, M_\xi^2). \quad (44)$$

2.1.6. Diagrams f and f′

Other topologies with two W bosons and one Goldstone in the loop are mentioned. The corresponding form factors are presented in the form of

$$\mathcal{A}_T^{(f+f')}(\xi) = \frac{g_{HWW}g_{ZWX}g_{AWX}}{16\pi^2 M_W^4}\Big[\mathcal{A}^T_{101}(\xi) + \mathcal{A}^T_{102}(\xi) + \mathcal{A}^T_{201}(\xi) + \mathcal{A}^T_{202}(\xi)\Big], \quad (45)$$

where the relevant terms are expressed in terms of Passarino–Veltman functions. The results read in detail as

$$\mathcal{A}^T_{101}(\xi) = (M_H^2 + 2M_W^2)\Big[C_{22} + C_{12} + C_2\Big](M_Z^2, 0, M_H^2, M_W^2, M_\xi^2, M_W^2) + 2M_W^2\Big[C_0 + C_1\Big](M_Z^2, 0, M_H^2, M_W^2, M_\xi^2, M_W^2), \quad (46)$$

$$\mathcal{A}_{102}^{T}(\xi) = [M_W^2(\xi-1) - M_H^2]\Big[C_{22} + C_{12}\Big](M_Z^2, 0, M_H^2, M_W^2, M_\xi^2, M_\xi^2)$$
$$- 2M_W^2\Big[C_0 + C_1\Big](M_Z^2, 0, M_H^2, M_W^2, M_\xi^2, M_\xi^2)$$
$$+ [M_W^2(\xi-3) - M_H^2]C_2(M_Z^2, 0, M_H^2, M_W^2, M_\xi^2, M_\xi^2), \tag{47}$$

$$\mathcal{A}_{201}^{T}(\xi) = [M_W^2(\xi-1) - M_H^2]\Big[C_{22} + C_{12}\Big](M_Z^2, 0, M_H^2, M_\xi^2, M_\xi^2, M_W^2)$$
$$+ [M_W^2(\xi+1) - M_H^2]C_2(M_Z^2, 0, M_H^2, M_\xi^2, M_\xi^2, M_W^2), \tag{48}$$

$$\mathcal{A}_{202}^{T}(\xi) = (M_H^2 - 2M_\xi^2)\Big\{C_{22} + C_{12} + C_2\Big\}(M_Z^2, 0, M_H^2, M_\xi^2, M_\xi^2, M_\xi^2). \tag{49}$$

2.1.7. Diagrams g and g′

Applying the same procedure, the form factors for diagrams g and g' are shown in this subsection. The results read

$$\mathcal{A}_T^{(g+g')}(\xi) = \frac{g_{HXX}g_{ZWX}g_{AWX}}{8\pi^2 M_W^2}\Big[\mathcal{A}_{010}^{T}(\xi) + \mathcal{A}_{020}^{T}(\xi)\Big]. \tag{50}$$

All terms in the equation are obtained:

$$\mathcal{A}_{010}^{T}(\xi) = \Big[C_{22} + C_{12} + C_2\Big](M_Z^2, 0, M_H^2, M_\xi^2, M_W^2, M_\xi^2), \tag{51}$$

$$\mathcal{A}_{020}^{T}(\xi) = -\Big[C_{22} + C_{12} + C_2\Big](M_Z^2, 0, M_H^2, M_\xi^2, M_\xi^2, M_\xi^2). \tag{52}$$

2.1.8. Diagrams h and h′

We also have

$$\mathcal{A}_T^{(h+h')}(\xi) = \frac{g_{HXX}g_{ZXX}g_{AXX}}{2\pi^2}\Big[C_{22} + C_{12} + C_2\Big](M_Z^2, 0, M_H^2, M_\xi^2, M_\xi^2, M_\xi^2). \tag{53}$$

2.1.9. Diagram i

We next have

$$\mathcal{A}_T^{(i)}(\xi) = 0. \tag{54}$$

2.1.10. Diagrams j and j′

Finally, we obtain

$$\mathcal{A}_T^{(j+j')}(\xi) = -\xi\,\frac{g_{Hcc}g_{Zcc}g_{Acc}}{4\pi^2}\Big[C_{22} + C_{12} + C_2\Big](M_Z^2, 0, M_H^2, M_\xi^2, M_\xi^2, M_\xi^2). \tag{55}$$

2.2. In 't Hooft–Veltman gauge

Summing all of the contributions listed in the previous subsection, we obtain the analytic results of the one-loop form factors needed to determine the decay amplitude $H \to Z\gamma$ in the general R_ξ. In this subsection, we set $\xi = 1$ corresponding to the 't Hooft–Veltman gauge. The form factors read in a compact form as follows:

$$(16\pi^2) \times \mathcal{A}_{21}^{T} = \Big\{4g_{ZWW}[(2d-3)g_{AWW}g_{HWW} + g_{AWX}g_{HWX}] - 4g_{Acc}g_{Hcc}g_{Zcc}$$

$$
\begin{aligned}
&+ 8g_{AXX}(g_{HWX}g_{ZWX} + g_{HXX}g_{ZXX})\Big\}[C_{22} + C_{12}](M_Z^2, 0, M_H^2, M_W^2, M_W^2, M_W^2) \\
&+ \Big\{4g_{ZWW}[(2d-3)g_{AWW}g_{HWW} + 3g_{AWX}g_{HWX}] - 4g_{Acc}g_{Hcc}g_{Zcc} \\
&+ 8g_{AXX}(3g_{HWX}g_{ZWX} + g_{HXX}g_{ZXX})\Big\}C_2(M_Z^2, 0, M_H^2, M_W^2, M_W^2, M_W^2) \\
&+ \Big(2g_{AWW}g_{HWW}g_{ZWW} - 8g_{AWW}g_{HWX}g_{ZWX} + 16g_{AWX}g_{HWX}g_{ZXX}\Big) \\
&\times C_2(M_H^2, M_Z^2, 0, M_W^2, M_W^2, M_W^2) \\
&+ \Big(10g_{AWW}g_{HWW}g_{ZWW} + 8g_{AWX}g_{HWX}g_{ZWW} + 16g_{AXX}g_{HWX}g_{ZWX}\Big) \\
&\times C_0(M_Z^2, 0, M_H^2, M_W^2, M_W^2, M_W^2). \qquad (56)
\end{aligned}
$$

2.3. In the unitary gauge

In the unitary gauge, we only take $\mathcal{A}_{111}^{(a+a')}$ and $\mathcal{A}_{11}^{(b)}$ into account. The result reads

$$
\begin{aligned}
(32\pi^2 M_W^4) \times \mathcal{A}_{21}^T = &\Big[2(M_H^2 + 2M_W^2)g_{AWW}g_{HWW}g_{ZWW} + 4(M_H^2 - M_W^2)g_{HWW}g_{ZAWW}\Big] \\
&\times B_{11}(M_H^2, M_W^2, M_W^2) \\
&+ 4M_W^2 g_{HWW}\big(g_{AWW}g_{ZWW} - g_{ZAWW}\big)B_0(M_H^2, M_W^2, M_W^2) \\
&+ 2g_{HWW}\Big[(M_H^2 + 2M_W^2)g_{AWW}g_{ZWW} - 2M_W^2 g_{ZAWW}\Big]B_1(M_H^2, M_W^2, M_W^2) \\
&+ 4g_{HWW}g_{ZAWW}\Big[M_H^2 B_{111} + B_{00} + 2B_{001}\Big](M_H^2, M_W^2, M_W^2) \qquad (57) \\
&+ 4g_{AWW}g_{HWW}g_{ZWW}\Big[2M_W^2(M_H^2 - M_Z^2) - M_H^2 M_Z^2 + 4(d-1)M_W^4\Big] \\
&\times [C_{22} + C_{12} + C_2](M_Z^2, 0, M_H^2, M_W^2, M_W^2, M_W^2) \\
&+ 8M_W^2\big(4M_W^2 - M_Z^2\big)g_{AWW}g_{HWW}g_{ZWW}C_0(M_H^2, M_Z^2, 0, M_W^2, M_W^2, M_W^2).
\end{aligned}
$$

In the limit $d \to 4$, the form factors in the three different gauges R_ξ, 't Hooft-Veltam and unitary are in the same simple form given as follows:

$$
\begin{aligned}
\mathcal{A}_{H\to Z\gamma}^{d\to 4} = &\frac{eg^2\cos\theta_W}{32\pi^2 M_H^2 M_W^3\left(M_H^2 - M_Z^2\right)^2}\left[2p_2^\mu p_1^\nu - (M_H^2 - M_Z^2)g^{\mu\nu}\right] \\
&\times \Bigg\{M_Z^2\sqrt{M_H^4 - 4M_H^2M_W^2}\left[M_H^2\left(2M_W^2 - M_Z^2\right) + 12M_W^4 - 2M_W^2M_Z^2\right] \\
&\times \ln\left[\frac{\sqrt{M_H^4 - 4M_H^2M_W^2} + 2M_W^2 - M_H^2}{2M_W^2}\right] \\
&+ M_H^2M_W^2\left[M_H^2\left(M_Z^2 - 6M_W^2\right) + 12M_W^4 + 6M_W^2M_Z^2 - 2M_Z^4\right] \\
&\times \ln^2\left[\frac{\sqrt{M_H^4 - 4M_H^2M_W^2} + 2M_W^2 - M_H^2}{2M_W^2}\right] \\
&+ M_H^2\sqrt{M_Z^4 - 4M_W^2M_Z^2}\left[M_H^2\left(M_Z^2 - 2M_W^2\right) + 2M_W^2\left(M_Z^2 - 6M_W^2\right)\right]
\end{aligned}
$$

$$\times \ln\left[\frac{\sqrt{M_Z^4 - 4M_W^2M_Z^2} + 2M_W^2 - M_Z^2}{2M_W^2}\right]$$
$$- M_H^2M_W^2\left[M_H^2\left(M_Z^2 - 6M_W^2\right) + 12M_W^4 + 6M_W^2M_Z^2 - 2M_Z^4\right]$$
$$\times \ln^2\left[\frac{\sqrt{M_Z^4 - 4M_W^2M_Z^2} + 2M_W^2 - M_Z^2}{2M_W^2}\right]$$
$$+ 2M_H^2M_W^2\left(M_H^2 - M_Z^2\right)^2 + M_H^2\left(12M_W^4 - M_H^2M_Z^2\right)\left(M_H^2 - M_Z^2\right)\Big\}. \quad (58)$$

By taking $M_Z^2 \to 0$ in Eq. (58), we then verify again many previous results for $H \to \gamma\gamma$; see Refs. [40,41] for examples. For W bosons exchanging in the loop, their masses are included in the Feynman's prescription as $M_W^2 - i\rho$. Therefore, all the above logarithmic functions are well-defined in the complex plane.

3. Numerical tests for the ξ-independence

Numerical illustrations of the form factors relating to the decay amplitude $H \to Z\gamma$ in different gauges are shown in Table 1. The last line of the table gives the numerical value of the form factors after taking out the coefficient $(eg^2)/(16\pi^2)$. The related masses are fixed as follows: $M_H = 125$ GeV, $M_Z = 91.2$ GeV and $M_W = 80.4$ GeV. We find that the results are well stable with different values $\xi = 0,\ 1,\ 100$ and $\xi \to \infty$.

The numerical result of the form factor in Eq. (21) (as a example of a numerical cross-check) of Ref. [20] is

$$\mathcal{F}_{21} = 0.07245981549100559\frac{eg^2}{16\pi^2}. \quad (59)$$

We find a perfect agreement between the result in this paper with that in Ref. [20].

4. Conclusions

The analytical results for the form factors presenting one-loop contributions of the W boson to the decay amplitude $H \to Z\gamma$ in the R_ξ gauge have been collected. They are expressed as functions of the Passarino–Veltman scalar coefficients such that numerical calculations are easily generated with `LoopTools`. In the limit of $d \to 4$, we have shown that these analytic results are independent of the unphysical parameter ξ and consistent with those given in previous works. Numerical checks for the ξ-independence of the form factors have also been discussed. In addition, the results are in good stability with varying $\xi = 0,\ 1,\ 100$ and $\xi \to \infty$. We emphasize that the results in this paper will be applied to calculate one-loop contributions of new charged gauge bosons appearing in many BSMs. They can be used to cross-check for consistency with well-known results given in the unitary gauge. This is another indirect way to confirm the new Goldstone boson couplings which often have complicated forms in the BSMs.

Acknowledgements

This research is funded by Vietnam National Foundation for Science and Technology Development (NAFOSTED) under the grant number 103.01-2019.346.

Table 1. Numerical checks for the ξ-independence of the form factors are studied.

Diagrams /ξ	$\xi \to 0$	$\xi = 1$	$\xi = 100$	$\xi \to \infty$
a	$0.05985185065310632 + 0.00467528078266156\,i$	0.06215891398415416	0.3209209899754058	$3.045808943133905 \times 10^{7}$
b	$-0.004780425280300761 - 0.012912138304675886\,i$	0	-0.2507738185381761	$-3.045808936065990 \times 10^{7}$
c	$0.01420681172938953 + 0.00618230306965115\,i$	0.011041675936102476	0.0011888522641987549	0.0005410399289955083
d	0	0	0	0
e	$0.003381779143108288 - 0.003941724009915961\,i$	0.0004225556213988878	0.00007343857541803593	0.00006391517156179955
f	$-0.005045377867037107 + 0.005184705008759242\,i$	0	0.0001476405256009515	0.0002619707739754035
g	$0.0001233773368155624 + 0.0008115734535198974\,i$	0	$1.0436687818979681 \times 10^{-6}$	$1.0553816412933658 \times 10^{-14}$
h	0.004721799775923751	-0.002769766130017844	-0.00001581903805520466	$-1.575446161278000 \times 10^{-13}$
i	0	0	0	0
j	$\mathcal{O}(10^{-23})$	0.001606436079367905	0.0009174880578314728	0.0009137426900957666
Sum	0.07245981549100559	0.07245981549100559	0.07245981549100559	0.07245981549100559

Funding

Open Access funding: SCOAP[3].

Appendix A. Feynman rules and Feynman diagrams

In this Appendix, we list the Feynman rules needed for writing all one-loop integrals contributing to the decay amplitude of the process $H \to Z\gamma$. All propagators and related couplings are shown in Tables A.1 and A.2, respectively.

Feynman diagrams for one-loop contributions to the decay amplitude $H \to Z\gamma$ in R_ξ gauge are plotted in Fig. A.1.

Table A.1. Feynman rules involving the decay $H \to Z\gamma$ through W boson loops in the R_ξ gauge.

Types	Propagators
Goldstone boson	$\dfrac{i}{p^2 - M_\xi^2}$
Ghost	$\dfrac{i}{p^2 - M_\xi^2}$
W boson	$\dfrac{-i}{p^2 - M_W^2}\left[g^{\mu\nu} - (1-\xi)\dfrac{p^\mu p^\nu}{p^2 - M_\xi^2}\right]$

Table A.2. All couplings involving the decay $H \to Z\gamma$ through W boson loops in the R_ξ gauge. The notations defining these couplings in the SM are: $g_{HWW} = gM_W$, $g_{HWX} = g/2$, $g_{HXX} = gM_H^2/(2M_W)$, $g_{Hcc} = gM_W/2$, $g_{AWW} = e$, $g_{ZWW} = -g\cos\theta_W$, $g_{AAWW} = e^2$, $g_{ZAWW} = -eg\cos\theta_W$, $g_{AWX} = eM_W$, $g_{ZWX} = gM_Z\sin^2\theta_W$, $g_{AXX} = e$, $g_{ZXX} = -g\cos 2\theta_W/(2\cos\theta_W)$, $g_{AAXX} = 2e^2$, $g_{ZAXX} = -eg\cos 2\theta_W/(\cos\theta_W)$, $g_{HAWX} = eg/2$, $g_{HZWX} = g^2\sin^2\theta_W/(2\cos\theta_W)$, $g_{Acc} = e$, $g_{Zcc} = -g\cos\theta_W$. The standard Lorentz tensors of the gauge boson self couplings are $\Gamma_{\mu\nu\lambda}(p_1,p_2,p_3) = g_{\mu\nu}(p_1-p_2)_\lambda + g_{\lambda\nu}(p_2-p_3)_\mu + g_{\mu\lambda}(p_3-p_1)_\nu$ and $S_{\mu\nu,\alpha\beta} = 2g_{\mu\nu}g_{\alpha\beta} - g_{\mu\alpha}g_{\nu\beta} - g_{\mu\beta}g_{\nu\alpha}$.

Vertices	Couplings
$H\cdot W_\mu\cdot W_\nu, H(p_1)\cdot W_\mu\cdot\chi(p_2), H\cdot\chi\cdot\chi, H\cdot c\cdot c$	$ig_{HWW}g_{\mu\nu}, -ig_{HWX}(p_2-p_1)_\mu, -ig_{HXX}, -i\xi g_{Hcc}$
$A_\mu(p_1)\cdot W_\nu^+(p_2)\cdot W_\lambda^-(p_3), Z_\mu(p_1)\cdot W_\nu^+(p_2)\cdot W_\lambda^-(p_3)$	$-ig_{AWW}\Gamma_{\mu\nu\lambda}(p_1,p_2,p_3), -ig_{ZWW}\Gamma_{\mu\nu\lambda}(p_1,p_2,p_3)$
$A_\mu\cdot A_\nu\cdot W_\alpha^+\cdot W_\beta^-, Z_\mu\cdot A_\nu\cdot W_\alpha^+\cdot W_\beta^-$	$-ig_{AAWW}S_{\mu\nu,\alpha\beta}, -ig_{ZAWW}S_{\mu\nu,\alpha\beta}$
$A_\mu\cdot W_\nu\cdot\chi, Z_\mu\cdot W_\nu\cdot\chi$	$-ig_{AWX}g_{\mu\nu}, -ig_{ZWX}g_{\mu\nu}$
$A_\mu\cdot\chi(p_1)\cdot\chi(p_2), Z_\mu\cdot\chi(p_1)\cdot\chi(p_2)$	$-ig_{AXX}(p_2-p_1)_\mu, -ig_{ZXX}(p_2-p_1)_\mu$
$A_\mu\cdot A_\nu\cdot\chi\cdot\chi, Z_\mu\cdot A_\nu\cdot\chi\cdot\chi$	$ig_{AAXX}g_{\mu\nu}, ig_{ZAXX}g_{\mu\nu}$
$H\cdot A_\mu\cdot W_\nu\cdot\chi, H\cdot Z_\mu\cdot W_\nu\cdot\chi$	$-ig_{HAWX}g_{\mu\nu}, -ig_{HZWX}g_{\mu\nu}$
$A_\mu\cdot c\cdot c, Z_\mu\cdot c\cdot c$	$-ig_{Acc}p_\mu, -ig_{Zcc}p_\mu$

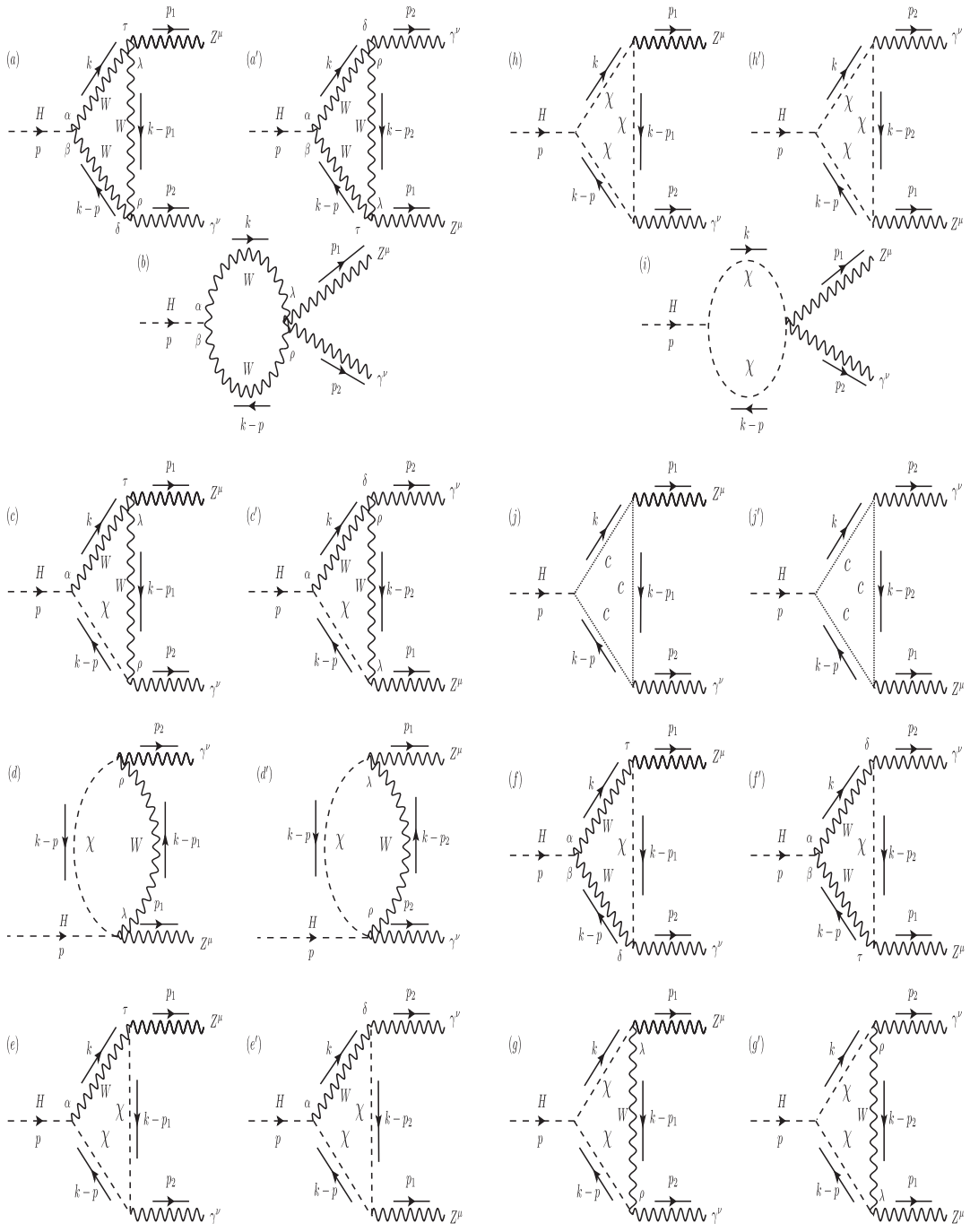

Fig. A.1. Feynman diagrams of one-loop W boson contributions to $H \to Z\gamma$ in R_ξ.

References

[1] V. M. Abazov et al. [DØ Collaboration], Phys. Lett. B **671**, 349 (2009).
[2] S. Chatrchyan et al. [CMS Collaboration], Phys. Lett. B **726**, 587 (2013).
[3] M. Aaboud et al. [ATLAS Collaboration], J. High Energy Phys. **1710**, 112 (2017).
[4] G. Aad et al. [ATLAS Collaboration], Phys. Lett. B **809**, 135754 (2020).
[5] R. N. Cahn, M. S. Chanowitz, and N. Fleishon, Phys. Lett. B **82**, 113 (1979).
[6] L. Bergström and G. Hulth, Nucl. Phys. B **259**, 137 (1985).
[7] R. Martínez, M. A. Pérez, and J. J. Toscano, Phys. Lett. B **234**, 503 (1990).
[8] A. Djouadi, V. Driesen, W. Hollik, and A. Kraft, Eur. Phys. J. C **1**, 163 (1998).
[9] A. Djouadi, J. Kalinowski, and M. Spira, Comput. Phys. Commun. **108**, 56 (1998).
[10] C.-W. Chiang and K. Yagyu, Phys. Rev. D **87**, 033003 (2013).
[11] C.-S. Chen, C.-Q. Geng, D. Huang, and L.-H. Tsai, Phys. Rev. D **87**, 075019 (2013).
[12] J. Cao, L. Wu, P. Wu, and J. M. Yang, J. High Energy Phys. **1309**, 043 (2013).
[13] R. Bonciani, V. Del Duca, H. Frellesvig, J. M. Henn, F. Moriello, and V. A. Smirnov, J. High Energy Phys. **1508**, 108 (2015).
[14] A. Hammad, S. Khalil, and S. Moretti, Phys. Rev. D **92**, 095008 (2015).
[15] G. Bélanger, V. Bizouard, and G. Chalons, Phys. Rev. D **89**, 095023 (2014).
[16] J. M. No and M. Spannowsky, Phys. Rev. D **95**, 075027 (2017).
[17] S. Taheri Monfared, Sh. Fayazbakhsh, and M. Mohammadi Najafabadi, Phys. Lett. B **762**, 301 (2016).
[18] D. Fontes, J. C. Romão, and J. P. Silva, J. High Energy Phys. **1412**, 043 (2014).
[19] S. Funatsu, H. Hatanaka, and Y. Hosotani, Phys. Rev. D **92**, 115003 (2015); **94**, 019902 (2016) [erratum].
[20] L. T. Hue, A. B. Arbuzov, T. T. Hong, T. P. Nguyen, D. T. Si, and H. N. Long, Eur. Phys. J. C **78**, 885 (2018).
[21] H. T. Hung, T. T. Hong, H. H. Phuong, H. L. T. Mai, and L. T. Hue, Phys. Rev. D **100**, 075014 (2019).
[22] M. Herrero and R. A. Morales, Phys. Rev. D **102**, 075040 (2020).
[23] A. Dedes, K. Suxho, and L. Trifyllis, J. High Energy Phys. **1906**, 115 (2019).
[24] T. Gehrmann, S. Guns, and D. Kara, J. High Energy Phys. **1509**, 038 (2015).
[25] I. Boradjiev, E. Christova, and H. Eberl, Phys. Rev. D **97**, 073008 (2018).
[26] K. H. Phan and D. T. Tran, Prog. Theor. Exp. Phys. **2020**, 053B08 (2020).
[27] J. C. Pati and A. Salam, Phys. Rev. D **10**, 275 (1974); **11**, 703 (1975) [erratum]
[28] R. N. Mohapatra and J. C. Pati, Phys. Rev. D **11**, 2558 (1975).
[29] G. Senjanovic and R. N. Mohapatra, Phys. Rev. D **12**, 1502 (1975).
[30] M. Singer, J. W. F. Valle, and J. Schechter, Phys. Rev. D **22**, 738 (1980).
[31] J. W. F. Valle and M. Singer, Phys. Rev. D **28**, 540 (1983).
[32] F. Pisano and V. Pleitez, Phys. Rev. D **46**, 410 (1992).
[33] P. H. Frampton, Phys. Rev. Lett. **69**, 2889 (1992).
[34] R. A. Diaz, R. Martinez, and F. Ochoa, Phys. Rev. D **72**, 035018 (2005) [arXiv:hep-ph/0411263] [Search INSPIRE].
[35] R. Foot, H. N. Long, and T. A. Tran, Phys. Rev. D **50**, R34(R) (1994) [arXiv:hep-ph/9402243] [Search INSPIRE].
[36] S.-P. He, Phys. Rev. D **102**, 075035 (2020).
[37] T. Hahn and M. Pérez-Victoria, Comput. Phys. Commun. **118**, 153 (1999).
[38] A. Denner and S. Dittmaier, Nucl. Phys. B **734**, 62 (2006).
[39] H. H. Patel, Comput. Phys. Commun. **197**, 276 (2015).
[40] W. J. Marciano, C. Zhang, and S. Willenbrock, Phys. Rev. D **85**, 013002 (2012).
[41] K. H. Phan and D. T. Tran, arXiv:2103.10045 [Search INSPIRE].